Journal of *Marine Science and Engineering*

MDPI

Article

Nitrate $\delta^{15}N$ and $\delta^{18}O$ Values Reveal Mariculture Impacts on Nitrogen Cycling in Sansha Bay, SE China

Jianpeng Li [1], Xuan Lu [1], Qingmei Zhu [2], Yanpei Zhuang [1,3,*], Wei Yang [1] and Di Qi [1,*]

[1] Polar and Marine Research Institute, College of Harbor and Coastal Engineering, Jimei University, Xiamen 361021, China; luke0401@163.com (J.L.); luxuan@jmu.edu.cn (X.L.); yangwei@jmu.edu.cn (W.Y.)
[2] College of Ocean and Meteorology, Guangdong Ocean University, Zhanjiang 524088, China; zhuqingmei1987@163.com
[3] Southern Marine Science and Engineering Guangdong Laboratory (Zhuhai), Zhuhai 519000, China
* Correspondence: zhuangyp@jmu.edu.cn (Y.Z.); qidi@jmu.edu.cn (D.Q.)

Abstract: Global fisheries' production has intensified rapidly over recent decades, making significant contributions to food security and economic development. However, this growth has exerted pressure on marine ecosystems and altered coastal nitrogen cycling. This study focused on Sansha Bay, an important aquaculture harbor in SE China, with measurements of environmental parameters and nitrate N–O isotopic compositions, to explore the impact of distinct mariculture types on nitrogen cycling in a coastal farming bay. The mean nitrate concentration was 120.7 ± 24.2 μmol dm^{-3}, with a mean N/P ratio of 69.6 ± 19.6, indicating that the water column is in a state of eutrophication. Different aquaculture practices influence the nutrient status of water, with mixed farming (shellfish, seaweed, and fish) increasing nitrate concentrations and reducing N/P ratios, while seaweed farming reduces nitrate concentrations and increases N/P ratios. In spring, the average $\delta^{15}N$ and $\delta^{18}O$ values of nitrate in the water column were 8.4‰ and 8.7‰, respectively, compared with values of 9.8‰ and 4‰ recorded previously in winter. Such variation may be attributed to the greater influence of seaweed farming in spring when nitrate cycling is driven mainly by assimilation. In terms of aquaculture type, nitrate assimilation was stronger in seaweed farming zones, and nitrification was more pronounced in mixed farming zones. Overall, the results demonstrate that different mariculture types in Sansha Bay influence nitrogen cycling in the water body, with seaweed-based aquaculture systems contributing to the sustainable development of marine aquaculture by effectively mitigating eutrophication.

Keywords: marine aquaculture; stable nitrogen isotopes; nitrate source; eutrophication; Sansha Bay

check for updates

Received: 16 January 2025
Revised: 5 February 2025
Accepted: 10 February 2025
Published: 13 February 2025

Citation: Li, J.; Lu, X.; Zhu, Q.; Zhuang, Y.; Yang, W.; Qi, D. Nitrate $\delta^{15}N$ and $\delta^{18}O$ Values Reveal Mariculture Impacts on Nitrogen Cycling in Sansha Bay, SE China. *J. Mar. Sci. Eng.* **2025**, *13*, 343. https://doi.org/10.3390/jmse13020343

Copyright: © 2025 by the authors. Licensee MDPI, Basel, Switzerland. This article is an open access article distributed under the terms and conditions of the Creative Commons Attribution (CC BY) license (https://creativecommons.org/licenses/by/4.0/).

1. Introduction

Nitrogen is an essential nutrient for life, and its cycling in coastal environments is influenced by complex fluid dynamics, biochemical processes, and human activity [1–5]. The input of reactive nitrogen (RN) into the human biosphere is estimated to have increased from 5.4 Tg N in 1980 to 15.4 Tg N in 2010 [6]. Phytoplankton growth in coastal waters is mainly limited by nitrogen and phosphorus, and elevated nitrogen and phosphorus concentrations can significantly increase phytoplankton biomass and growth rate [7]. Excess nitrogen input into the oceans has triggered a range of ecological and environmental consequences in coastal waters, including eutrophication, seasonal hypoxia, and algal blooms [8–11]. The tracking of nitrogen sources and an understanding of nitrogen cycling processes in coastal ecosystems are thus vital to the remediation of such problems.

With the increasing global demand for seafood, fisheries and aquaculture are expanding rapidly. Between 2000 and 2019, global aquaculture production increased from 43 million tons to 120.1 million tons, representing an increase of nearly 180% [12]. Since 1970, ~2.1 Tg N has been introduced into aquatic environments annually through aquaculture feed [13], seriously impacting coastal nitrogen cycling [14,15]. Previous studies have indicated that nitrogen cycling in aquacultural areas may be closely related to the type of aquaculture practiced [16,17]. For example, in fish farming areas, feed conversion efficiency is only 20–25% [18], resulting in the accumulation of substantial amounts of unabsorbed nutrients and waste in the water [19–21]. This accumulation may lead to hypoxic conditions in sediments and promote ammonium (NH_4^+) production [22]. In contrast, in seaweed farming areas, seaweed reduces nutrient concentrations in the water, converting nutrients to valuable algal biomass, thereby improving water quality and alleviating eutrophication [23–26]. With the rapidly growing marine aquaculture industry in China, and its complex and unique systems in coastal farming, analysis of the impacts of different types of aquacultures on nitrogen transformation and migration is essential.

Dual isotopic measurements on dissolved nitrate ($\delta^{15}N\text{-}NO_3^-$ and $\delta^{18}O\text{-}NO_3^-$ values) have become powerful tools in elucidating nitrogen sources and transformation processes in marine systems [27–40]. Different nitrogen sources can be differentiated on the basis of their distinct nitrate (NO_3^-) dual isotopic compositions [41,42]. For example, nitrogen derived from manure and sewage typically has higher $\delta^{15}N$ values (10‰–20‰), while $\delta^{15}N$ values in soil, fertilizers, and atmospheric deposition are lower (−5‰ to +10‰) [41,42]. The $\delta^{18}O$ values of atmospheric deposition (>50‰) are much higher than those associated with other oxygen sources (<25‰) [43]. Consequently, dual NO_3^- isotopic compositions are used extensively in tracing biogeochemical processes such as nitrification, denitrification, N_2 fixation, and phytoplankton assimilation. During assimilation and denitrification, phytoplankton and microorganisms preferentially absorb lighter isotopes (^{14}N and ^{16}O), leading to the enrichment of ^{15}N and ^{18}O in residual nitrate in the water column [44–46]. Nitrification reduces nitrate $\delta^{15}N$ values, while organic nitrogen produced through N_2 fixation may increase the proportion of ^{14}N in seawater during remineralization [47]. Bayesian models can be used to quantify the relative contributions of different nitrogen sources to seawater, based on their isotopic signatures, thereby identifying the major sources of pollution [1,4,48,49]. Lao et al. found that the primary sources of nitrate along the western coast of Guangdong Province are fecal matter and wastewater [1]. This indicates that, despite the westward flow of diluted water from the Pearl River, the nitrate levels in the coastal areas of western Guangdong are primarily influenced by local urban activities. These findings provide a scientific basis for regional water quality management. Coupled processes of nitrification and denitrification play crucial roles in controlling the dynamics and fate of nitrate in estuarine and coastal environments [50]. Therefore, a deeper understanding of nitrogen sources and nitrogen cycling in the marine environment can be achieved by the analysis of dual NO_3^- isotopic compositions.

Sansha Bay in SE China is home to a long-standing integrated multi-nutrient aquaculture base [51]. The bay is renowned for its seaweed-based marine aquaculture systems, with the large yellow croaker (*Larimichthys crocea*) being the main species cultivated [52]. Due to natural geographic conditions and the impact of intensive marine aquaculture, the water turnover time in the main channel of Sansha Bay is <10 days, while in the upstream area of the bay, it exceeds 30 days [53]. Sansha Bay thus provides an ideal setting for studying the effects of mixed marine aquaculture systems on nitrogen cycling. However, research on the nitrogen cycle and nitrate sources in Sansha Bay, particularly involving dual isotopes, has been limited to date. Here, we determined hydrologic parameters (salinity and temperature), nutrient concentrations, and dual nitrate isotopes ($\delta^{15}N\text{-}NO_3^-$ and

δ^{18}O-NO_3^- values) for the waters of Sansha Bay during the spring of 2024, referencing historical data from the winter of 2021 [49]. A Bayesian stable-isotope mixing model was employed to identify nitrate sources. Through these analyses, we aimed to assess the impact of different aquaculture activities on nitrogen and oxygen isotopic compositions in Sansha Bay and to identify the primary nitrate sources. This study found that optimizing aquaculture management practices, particularly through the selection of feed types, can enhance production efficiency in aquaculture, thereby reducing farming costs and nitrogen emissions, which in turn mitigates the phenomenon of water eutrophication. This research provides a practical foundation for sustainable development and promotes the adoption of environmentally friendly aquaculture practices.

2. Materials and Methods

2.1. Study Area and Sampling

A survey was undertaken in Sansha Bay (Figure 1) in the spring of 2024 (4–8 April) during heavy rainfall. This time period may not capture long-term dynamics due to the time constraints of data sampling; however, it is still applicable to studies of short-term changes. Water samples were collected at 40 sampling stations using 5 L Niskin bottles, and sea surface temperature (SST) and salinity (SSS) were recorded. Hydrological parameters, including temperature and salinity, were measured using a conductivity–temperature–depth (CTD) recorder (SBE19plus, Sea-bird, Bellevue, WA, USA). Depending on the water depth, two layers (for depths of <40 m) or three layers (>40 m) of water samples were collected at each sampling point. 'Surface' water refers to the water column within 1 m of the surface, and 'bottom' water refers to the column within 1 m of the seafloor.

Sansha Bay lies on the northeastern coast of Fujian Province (Figure 1), covering an area of ~675 km^2 and comprising several secondary bays such as Dongwuyang and Sandu'ao. Water chemistry parameters and their spatiotemporal distributions in Sansha Bay are affected by intensive aquaculture activities [51]. Water masses may play an important role in nutrient cycling and the ecological environment in coastal areas [54]. Groundwater inputs also contribute to nutrient fluxes within the bay [51].

Based on survey observational data and a 2022 aquaculture map for Sansha Bay [55], we categorized the study area into three zones: seaweed farming, mixed farming (shellfish and fish), and non-farming. Seaweed farming occurs mainly in the northeastern inner bay, with only a minor presence in the estuary; mixed farming occurs in the central part of the main channel and inner bay; and the non-farming zone is located in the main channel region (Figure 1).

2.2. Nutrient Analysis

Nutrient samples were filtered through pre-combusted glass-fiber filters (47 mm diameter, Whatman GF/F) after treatment at 450 °C for 5 h. The filtrate was transferred to acid-washed polyethylene bottles and stored at –20 °C. Nutrient NO_3^-, nitrite (NO_2^-), NH_4^+, PO_4^{3-}, and $Si(OH)_4$ concentrations were determined using a San++ continuous-flow analyzer (Skalar, Breda, The Netherlands), with detection limits of 0.1, 0.05, 0.05, 0.05, and 0.05 μmol dm^{-3}, respectively.

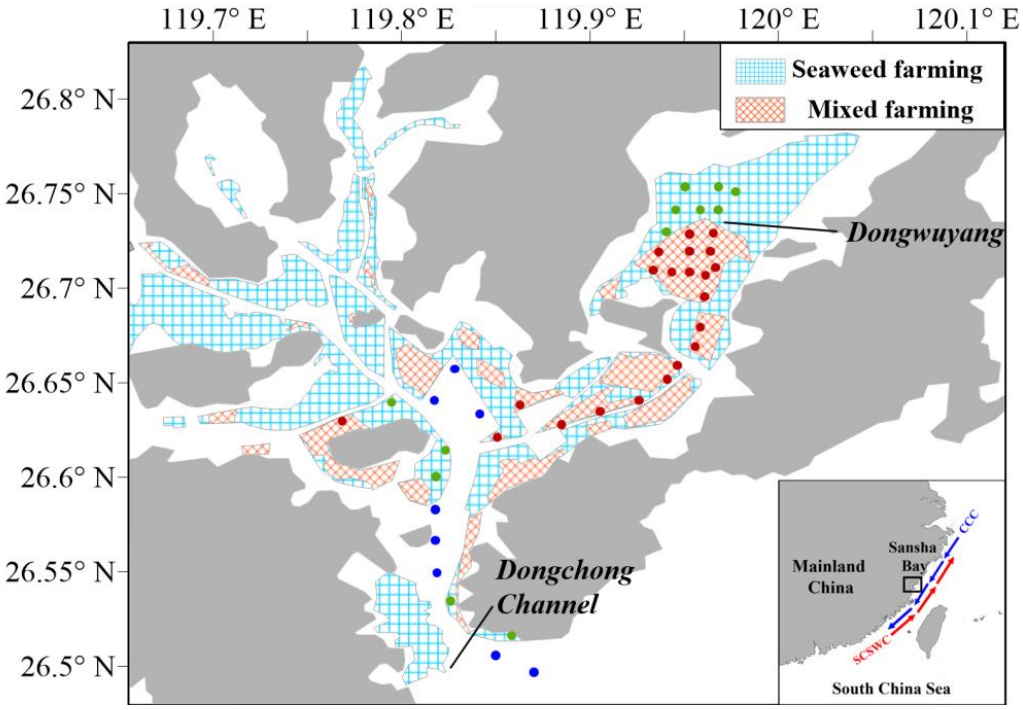


Figure 1. Locations of sampling stations and aquaculture farms in Sansha Bay. Solid green, red, and blue circles represent sampling stations in the seaweed farming zone, mixed farming zone, and non-farming zone (main navigation channel), respectively. The inset shows the location of Sansha Bay and offshore ocean currents, with the China Coastal Current (CCC, blue arrow) being active in winter and the South China Sea Warm Current (SCSWC, red arrow) being active in summer [56].

2.3. Isotopic Analysis

The δ^{15}N-NO_3^- and δ^{18}O-NO_3^- values were determined by a chemical-reduction method [57]. Given that the isotopic composition of NO_2^- may differ significantly from that of NO_3^-, and that the fractionation associated with the conversion of NO_2^- to N_2O is distinct from that of NO_3^- conversion, neglecting the presence of NO_2^- could lead to erroneous interpretations [32]. First, NO_2^- was removed from seawater using sulfamic acid [58]; NO_3^- was reduced to NO_2^- using sponge-like Cd, followed by a further reduction to N_2O with sodium azide buffered to pH 4–5 with acetic acid; N_2O was then isolated and purified; and δ^{15}N and δ^{18}O values were determined by gas chromatography–mass spectrometry (GCMS) using GasBench II-AT 253 Plus (Thermo Fisher Scientific, Waltham, MA, USA). Standard deviations for δ^{15}N and δ^{18}O values were <0.2‰ and <0.5‰, respectively. Calibrations were performed using the international standard IAEA-N3. The reproducibility of repeated determinations of δ^{15}N and δ^{18}O was within 0.3‰ (mean ± 0.1‰) and 0.6‰ (mean ± 0.3‰), respectively. The isotope analysis method in this study is consistent with that of Bu et al. [49].

2.4. Bayesian Model

The contributions of potential sources to nitrate concentrations in the sampled water were quantified using a Bayesian mixing model implemented in the R package SIAR (version 4.1.2). This model has been widely used in estimating the proportional contributions of various nitrate sources [1,48,59–62]. The framework of the model is as follows [42,63]:

$$X_{ij} = \sum_{k=1}^{k} P_k\left(S_{jk} + c_{jk}\right) + \epsilon_{ij}, \quad (1)$$

$$S_{jk} \sim N\left(\mu_{jk}, \omega_{jk}^2\right) \quad (2)$$

$$c_{jk} \sim N\left(\lambda_{jk}, \tau_{jk}^2\right) \quad (3)$$

$$c_{jk} \sim N\left(\lambda_{jk}, \tau_{jk}^2\right) \quad (4)$$

where X_{ij} and S_{jk} represent the dual isotopic values for NO_3^- in the mixed sample and for NO_3^- in the source, respectively; μ_{jk} and ω_{jk}, respectively, denote the mean and standard deviation of the normal distribution for S_{jk}; P_k indicates the proportional contribution of source k; c_{jk} is the fractionation factor for the dual NO_3^- isotopes in source k; λ_{jk} and τ_{jk}, respectively, represent the mean and standard deviation of the normal distribution for c_{jk}; and ϵ_{jk} accounts for the residuals of unquantified variation between individual samples, where 0 and σ_j^2 denote the normal distribution of ϵ_{jk}. Details of the model are provided by Moore and Semmens, 2008 [63], Xue et al., 2009 [42], and Zhang et al., 2018 [60].

3. Results

During the 2024 spring survey, the water depth in the Sansha Bay study area ranged from 3 to 60 m, and SST ranged from 16.1 °C to 20.5 °C (average 16.97 ± 1.11 °C). The highest water temperatures were recorded in nearshore areas of the bay, and the lowest water temperatures were recorded in the estuary outside the bay (Figure 2b). The SSS ranged from 28.83 to 31.13 (average 29.67 ± 0.58). In contrast to temperature, the highest salinity was recorded in the estuary, and the lowest was recorded in nearshore areas of the bay (Figure 2c). Surface concentrations (μmol dm^{-3}) of NO_3^- ranged from 55.5 to 159.3 (average 120.7 ± 24.2); NH_4^+, from 0.14 to 8.73 (3.40 ± 2.26); PO_4^{3-}, from 0.63 to 3.16 (1.94 ± 0.65); and $Si(OH)_4$, from 13.9 to 30.5 (24.2 ± 3.8). Nutrient concentrations in both surface and bottom waters in the estuary of Sansha Bay were lower than those in central areas of the bay, implying that the input of offshore seawater may not be the primary source of nutrients (Figure 2d–f and Figure S1). In spring, river runoff enters Sansha Bay, where another area with relatively low surface nutrient concentrations was identified at the western river estuary. This observation suggests that the input of riverine nutrients during spring has a minimal impact on the nutrient levels in Sansha Bay. N/P ratios ranged from 40.9 to 130.6 (average 69.6 ± 19.6), peaking in the nearshore Dongwuyang area and reaching their lowest values in the central mixed aquaculture zone (Figure 2g). The N/Si ratio in the water column ranged from 3.7 to 6.5 (average 5.2 ± 0.6) (Figure S1). $\delta^{15}N\text{-}NO_3^-$ values ranged from 6.1‰ to 14.5‰ (average 8.4‰ ± 1.46‰), and $\delta^{18}O\text{-}NO_3^-$ values ranged from 6.5‰ to 15.3‰ (8.7‰ ± 1.7‰), with the highest values recorded in the Dongwuyang nearshore seaweed farming zone, and the lowest values recorded in the central mixed farming zone (Figure 2h,i).

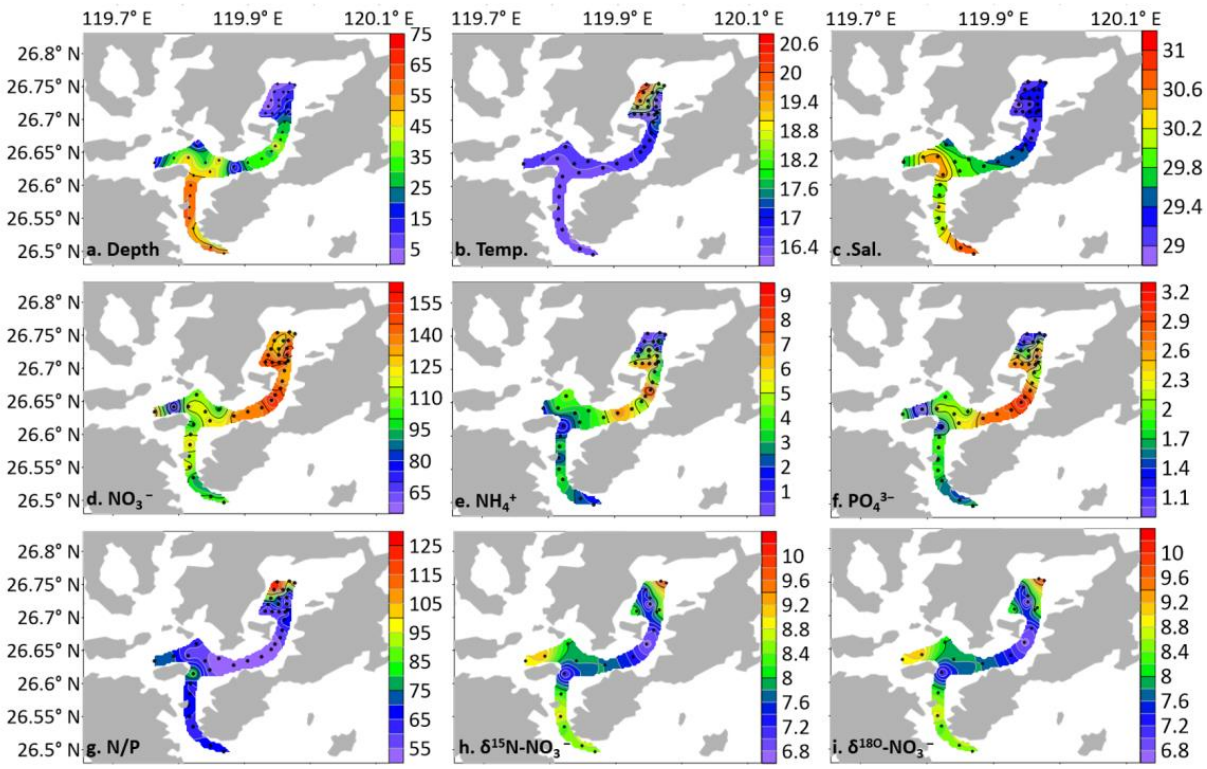


Figure 2. (**a**) Station depth (m) and average sea surface (**b**) temperature (°C), (**c**) salinity, (**d**) NO_3^- concentration (μmol dm^{-3}), (**e**) NH_4^+ concentration (μmol dm^{-3}), (**f**) PO_4^{3-} concentration (μmol dm^{-3}), (**g**) NO_3^-/PO_4^{3-} ratio, (**h**) $\delta^{15}N\text{-}NO_3^-$ value (‰), and (**i**) $\delta^{18}O\text{-}NO_3^-$ value (‰) in Sansha Bay during spring 2024.

4. Discussion

4.1. Impact of Aquaculture Type on Nutrient Levels

Nutrient concentrations in the surveyed area indicate high nitrate stress related to eutrophication, as assessed by coastal eutrophication evaluation criteria [64] (Table S1). The water in Sansha Bay is characterized by excessive inorganic nitrogen levels, whereas there is weaker nutrient stress due to phosphorus. The average water N/P ratio during spring exceeded 70, compared with an average of 14.3 in winter 2021 [49]. The high N/P ratio is likely attributable to increased aquaculture activity in spring, with substantial feed input enhancing NH_4^+ levels and promoting nitrification processes that generate nitrate [65]. Higher spring water temperatures and abundant sunlight likely enhanced the metabolic activity of nitrifying bacteria, increasing the rate of nitrification [66]. Higher nutrient concentrations were observed in the inner part of Sansha Bay, decreasing towards the outer bay (Figure 2). Nutrient sources are mainly related to local aquaculture activities, with excessive nitrogen inputs from anthropogenic sources contributing to eutrophication.

A one-way ANOVA analysis was undertaken for data from the seaweed farming, mixed farming, and non-farming zones using SPSS software v. 26. The results indicate significant differences in nutrient concentrations and nutrient ratios between the three zones ($p < 0.005$; Table S3), suggesting differences in nutrient sources and cycling and validating the rationale for the zonation. The mixed farming zone had the highest nutrient levels, with average NO_3^-, NH_4^+, and PO_4^{3-} concentrations of 133.2, 5.09, and 2.45 μmol dm^{-3}, respectively (Figure 3). Millions of tons of feed are applied annually to support fish farming in Sansha Bay [67], with 5–10% decomposing in the water [68], thereby releasing large amounts of nitrogen. Previous studies have shown that farming *L. crocea* and shellfish results in substantial increases in inorganic nitrogen concentrations

in marine environments [69]. Aquaculture activities, particularly the feeding of *L. crocea*, are thus likely the primary contributors to elevated nutrient concentrations in the mixed farming zone. Conversely, the seaweed culture zone had the lowest nutrient concentrations, with average NO_3^-, NH_4^+, and PO_4^{3-} concentrations of 110.7, 1.46, and 1.30 μmol dm^{-3}, respectively, significantly lower than those of the mixed farming and non-farming zones. This may be attributed to substantial nutrient uptake during algal growth [70].

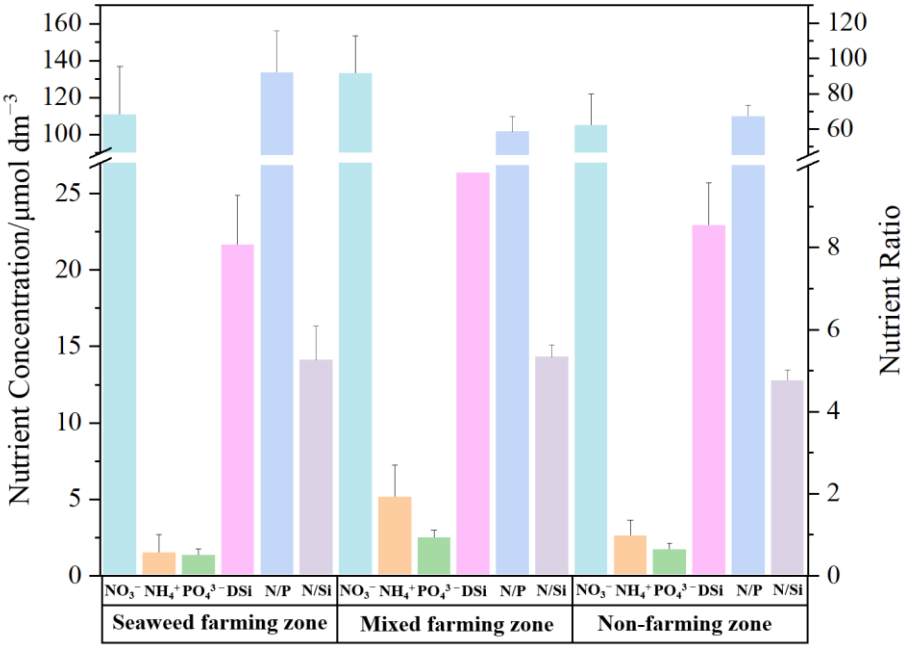


Figure 3. Comparison of nutrient parameters in the water column across different aquaculture types in Sansha Bay during spring 2024.

The seaweed farming zone had an average N/P ratio of 91.8 compared with 67.1 in the non-farming zone and 58.3 in the mixed farming area (Figure 3). These differences may be related to aquaculture type. Zhang et al., 2022 [16] reported that bivalve and seaweed farming remove N and P at ratios of 35:1 and 12:1, respectively. In mixed farming zones, bivalve cultivation may thus reduce water N/P ratios through harvesting. In contrast, seaweed farming tends to increase N/P ratios, as found by Zhang et al., 2022 [16] and Bu et al., 2024 [49]. The higher N/P ratios in the seaweed farming area may also be associated with groundwater discharge, as fresh submarine groundwater is a significant source of nutrients entering coastal waters, with N/P ratios of up to 585 [71].

Our results thus indicate that mixed farming increases dissolved inorganic nitrogen (DIN) concentrations while reducing N/P ratios, whereas seaweed farming reduces DIN concentrations and raises N/P ratios. The main difference between the seaweed and mixed farming zones is *L. crocea* and shellfish cultivation, both of which influence nutrient distributions [69,72] and alter nitrate conversion processes. The higher DIN concentration in mixed farming zones is likely due to low rates of feed utilization [73]. Currently, the primary feed types for large yellow croakers in Sansha Bay are categorized as trash fish feed and formulated feed. The nitrogen utilization efficiency of the trash fish feed system is relatively low (20.6%), resulting in a greater release of nitrogen into the environment. In contrast, the formulated feed system demonstrates better nitrogen utilization, with an efficiency of 32.5%, thereby exerting a lesser negative impact on the environment [69]. Improved methods of feed application are thus crucial for the mitigation of water eutrophication.

4.2. Impact of Aquaculture on N and O Isotopic Compositions

Aquaculture activities in Sansha Bay are typically more intense in spring than in winter, with winter generally being the 'seedling' season and spring being the peak season [74]. Therefore, we compared the relationships between nitrate $\delta^{15}N$ and $\delta^{18}O$ values in the water column during spring and winter, with winter data sourced from Bu et al., 2024 [49]. We obtained significant positive linear correlations between $\delta^{15}N$ and $\delta^{18}O$ for both seasons, with $R^2 = 0.6$ in spring and $R^2 = 0.53$ in winter, with respective regression gradients of 0.96 and 0.74 (Figure 4). Previous studies have indicated that assimilation processes affect $\delta^{15}N\text{-}NO_3^-$ and $\delta^{18}O\text{-}NO_3^-$ values similarly, resulting in a gradient of 1 in linear regression analysis [44,45]. In contrast, denitrification enriches residual nitrate, resulting in a $\delta^{15}N$:$\delta^{18}O$ value of 2 [41,75]. This seasonal difference may be attributed to vigorous seaweed cultivation activities in spring, enhancing nitrate assimilation. Denitrification is highly active in sediments [76], and the strong denitrification observed in sediments of Sansha Bay during winter [49] is likely related to the abundant organic matter provided by biological production and the deposition of organic debris on the seafloor [77,78].

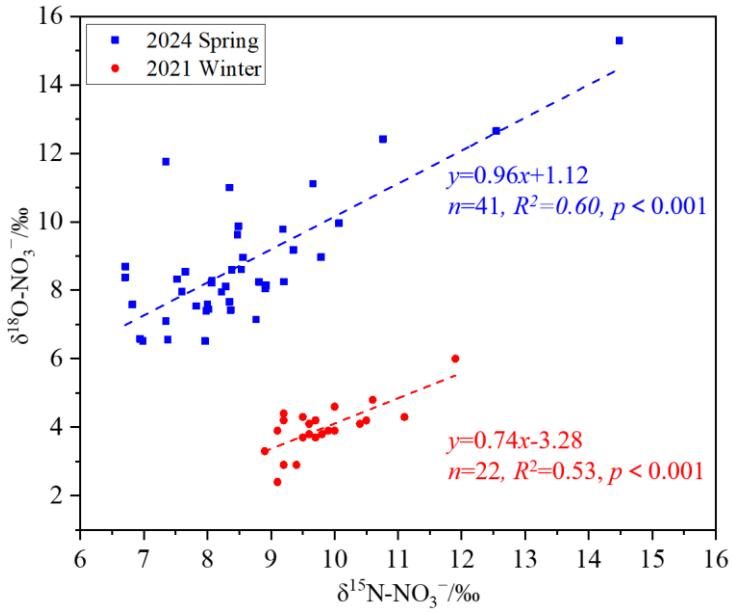


Figure 4. Relationship between $\delta^{15}N\text{-}NO_3^-$ and $\delta^{18}O\text{-}NO_3^-$ (‰) in surface water in Sansha Bay during spring 2024 and winter 2021.

The nitrate $\delta^{15}N$ and $\delta^{18}O$ values show significant differences between zones (Table S3), with average values decreasing in the following order: seaweed farming (9.72‰ and 10.25‰, respectively), non-farming (8.43‰ and 8.35‰), and mixed farming (7.81‰ and 7.97‰) (Figure 5). Denitrification and algal assimilation processes thus lead to enrichments in ^{15}N and ^{18}O, with algae and microbes preferentially absorbing the lighter isotopes ^{14}N and ^{16}O [46,79,80]. Conversely, nitrification tends to reduce ^{15}N levels, with microbes preferentially utilizing ^{14}N to produce nitrates [47]. The high levels of dissolved oxygen (>6.5 mg dm^{-3}) in the waters of Sansha Bay during the study period indicate that denitrification is unlikely to have occurred. Therefore, the elevated $\delta^{15}N$ and $\delta^{18}O$ values and low nitrate levels in the seaweed farming zone can be attributed to algal assimilation processes (Figure 5). The low $\delta^{15}N$ values in the mixed farming zone may be due to nitrification, as indicated by the substantial production of nitrates in this area. The farming of *L. crocea* in the mixed farming zone requires the provision of large quantities of feed rich in nutrients, resulting in elevated NH_4^+ levels (Figure 3) that may promote nitrification [79]. In contrast,

the seaweed farming zone had significantly lower NH_4^+ concentrations (Figure 3), which may enhance phytoplankton assimilation [81].

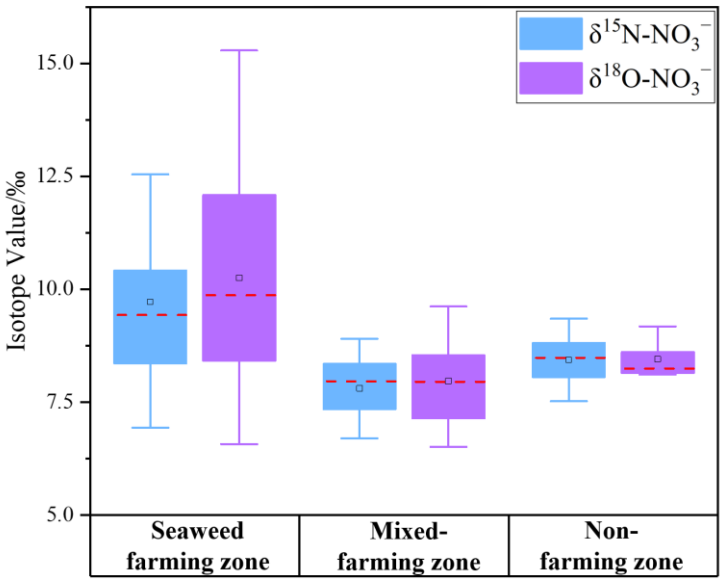


Figure 5. $\delta^{15}N\text{-}NO_3^-$ and $\delta^{18}O\text{-}NO_3^-$ values across the three aquaculture zones (seaweed farming, mixed farming, and non-farming) during spring 2024. The red dashed line represents the median line.

4.3. Nitrate Sources in the Different Aquaculture Zones

Our analyses indicate that excessive nitrogen input has led to eutrophication in the study area, the mitigation of which relies on the identification of nitrogen sources. Based on the dual-isotope method for the identification of nitrate sources [41,42], $\delta^{15}N\text{-}NO_3^-$ and $\delta^{18}O\text{-}NO_3^-$ values in the waters of Sansha Bay suggest that the primary sources of nitrate are manure and sewage (Figure 6), as indicated by the relatively positive $\delta^{15}N\text{-}NO_3^-$ values, although other major sources include reduced-N fertilizers, soil nitrogen, and atmospheric deposition [82]. The relative contributions of these four potential sources have been assessed in many studies [1,60,63,83]. We used the observed $\delta^{15}N\text{-}NO_3^-$ and $\delta^{18}O\text{-}NO_3^-$ values and the Bayesian mixing model to estimate nitrate source contributions [84], as shown in Table S2.

The results of Bayesian modeling indicate that the primary sources of nitrate in the waters of Sansha Bay in April 2024 were manure and sewage, accounting for 53% of the total, followed by soil organic nitrogen (28%), reduced-N fertilizers (11%), and atmospheric deposition (8%). There were significant differences in nitrate sources across the different aquaculture zones. In the seaweed farming zone, manure and sewage contributed the highest proportion of nitrate sources (64%), followed by the non-farming and mixed farming zones (Figure 7). This result is consistent with the inference that the seaweed farming zone may be receiving sewage input, leading to elevated seawater temperatures and high N/P ratios. The highest concentrations of soil organic nitrogen and nitrogen fertilizers were found in the mixed farming zone (31% and 16%, respectively), which is related to the farming of *L. crocea*. The feed for mixed fish contains a significant amount of nitrogen, of which only ~20.6% is converted to fish biomass; the rest is lost to the water in dissolved and particulate forms [69]. Compared with the analysis of nitrate sources in winter 2021 [49], there was a marked increase in nitrate from atmospheric deposition during the spring survey period, likely due to heavy rainfall in Sansha Bay during April 2024, with the deposition of substantial amounts of nitrate into surface waters [60]. According to the study by Chen et al., 2022 [48], in Qinzhou Bay, which experiences river input, the contributions of soil nitrogen (30%) and fertilizers (24%) are higher compared to the eastern

region of Sansha Bay, which has lower river input (28% and 11%, respectively). Conversely, the contributions from fecal matter and wastewater in Sansha Bay (53%) exceed those in Qinzhou Bay (41%). This indicates that in coastal bays with river input, rivers can transport substantial amounts of terrestrial pollutants to nearshore marine areas, while in estuaries without river input, the pollution reflects the impacts of aquaculture activities or the discharge of urban fecal matter and wastewater.

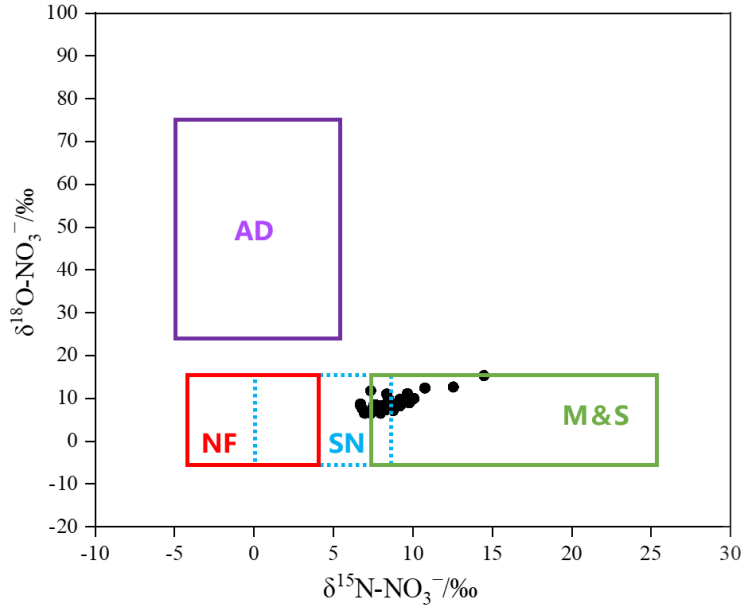


Figure 6. Relationship between δ^{15}N-NO_3^- and δ^{18}O-NO_3^- values in Sansha Bay (black dots) during spring 2024. End-member values for potential NO_3^- sources are from Kendall et al., 2007 [85] and Zhang et al., 2018 [60]. SN = soil organic N; M&S = manure and sewage; NF = nitrogen fertilizer; AD = atmospheric deposition.

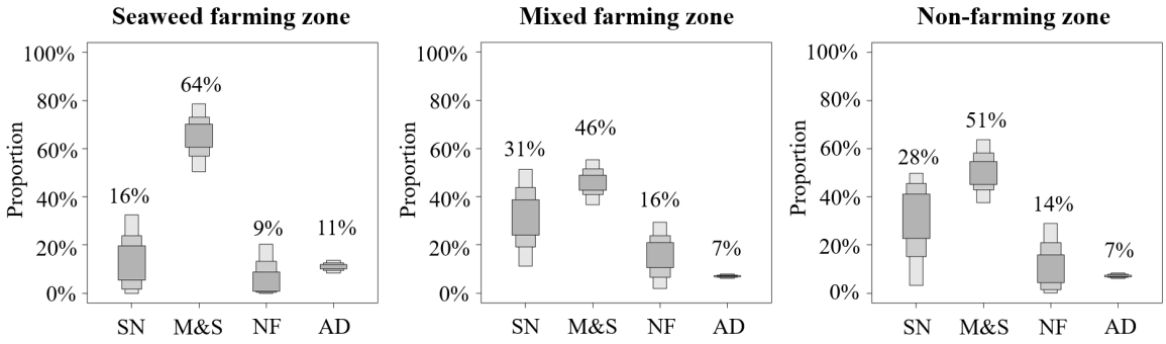


Figure 7. Relative contributions of four potential sources of nitrate in the water of Sansha Bay across various sampling regions during spring 2024. SN = soil organic N; M&S = manure and sewage; NF = nitrogen fertilizer; AD = atmospheric deposition.

5. Conclusions

During the spring survey of Sansha Bay, the average concentrations of NO_3^- and NH_4^+ in water were 120.7 and 3.40 μmol dm^{-3}, respectively, with an average N/P ratio of 69.6. These values indicate that the water is in a state of eutrophication, with a higher degree of eutrophication in spring than in winter, likely due to intensified aquaculture activities and feed input during spring. These results indicate that aquaculture plays a significant role in eutrophication. Aquacultural areas in Sansha Bay were categorized as seaweed, mixed, and non-farming zones. Statistical tests revealed significant differences in nutrient concentrations, nutrient ratios, and δ^{15}N-NO_3^- and δ^{18}O-NO_3^- values among

these zones ($p < 0.005$). Water nutrient concentrations vary with aquaculture type, with mixed farming resulting in higher DIN concentrations and lower N/P ratios, and seaweed farming resulting in lower DIN concentrations and higher N/P ratios. Average NO_3^- $\delta^{15}N$ and $\delta^{18}O$ values in the bay water in spring were 8.4‰ and 8.7‰, respectively, compared with winter values of 9.8‰ and 4‰. Nitrate $\delta^{15}N$-$\delta^{18}O$ correlations across the two seasons revealed significant positive linear relationships, with regression gradients of 0.96 in spring and 0.55 in winter. This indicates that in spring, the biogeochemical cycling of nitrate is driven primarily by assimilation, while denitrification is the dominant process in winter. Areas with algal cultivation exhibited stronger assimilation of nitrate, and mixed farming areas are characterized by greater nitrification. Our analysis indicated that excessive nitrogen input has led to eutrophication in the study area, thereby highlighting the role of different mariculture types in Sansha Bay on the nitrogen cycling of the water body, with seaweed-based aquaculture systems contributing to the sustainable development of mariculture by absorbing nitrate.

Supplementary Materials: The following supporting information can be downloaded at https://www.mdpi.com/article/10.3390/jmse13020343/s1, Figure S1. Spatial distribution of (a) NO_2^- (μmol dm^{-3}), (b) $Si(OH)_4$ (μmol dm^{-3}), and (c) N/Si in Sansha Bay during the spring of 2024; Table S1. Evaluation indicators and classification standards for nutrient stress related to eutrophication in coastal waters; Table S2. The Isotope Values (range and mean, ‰) of Potential Nitrate Sources for the River Mouth in Literature; Table S3. Significant differences in various parameters among different aquaculture zones.

Author Contributions: Methodology, X.L., Q.Z. and Y.Z.; Investigation, J.L., X.L. and W.Y.; Writing—original draft, J.L.; Writing—review & editing, Y.Z.; Funding acquisition, Y.Z. and D.Q. All authors have read and agreed to the published version of the manuscript.

Funding: This work was supported by the National Key Research and Development Program of China (2023YFC3108102), the National Natural Science Foundation of China (42376251), the Fujian Provincial Science and Technology Plan & Natural Science Foundation of Fujian Province (2023J06036), and the Fujian Provincial Department of Education—Sea Economy government, industry, University and research alliance (FOCAL2023-0101) the Ocean Negative Carbon Emissions (ONCE) Program.

Institutional Review Board Statement: Not applicable.

Informed Consent Statement: Not applicable.

Data Availability Statement: The original contributions presented in this study are included in the article/Supplementary Materials. Further inquiries can be directed to the corresponding author(s).

Acknowledgments: We would like to thank Chunqing Chen, Qiyao Zhao, and Hui Zeng for their support in sample measurement. We are grateful to all members of the Polar and Marine Research Institute, Jimei University, for their logistical support.

Conflicts of Interest: The authors declare no conflict of interest.

References

1. Lao, Q.; Chen, F.; Liu, G.; Chen, C.; Jin, G.; Zhu, Q.; Wei, C.; Zhang, C. Isotopic evidence for the shift of nitrate sources and active biological transformation on the western coast of Guangdong Province, South China. *Mar. Pollut. Bull.* **2019**, *142*, 603–612. [CrossRef]
2. Yang, B.; Gao, X.; Zhao, J.; Lu, Y.; Gao, T. Biogeochemistry of dissolved inorganic nutrients in an oligotrophic coastal mariculture region of the northern Shandong Peninsula, north Yellow Sea. *Mar. Pollut. Bull.* **2020**, *150*, 110693. [CrossRef] [PubMed]
3. Chen, F.; Lao, Q.; Zhang, S.; Bian, P.; Jin, G.; Zhu, Q.; Chen, C. Nitrate sources and biogeochemical processes identified using nitrogen and oxygen isotopes on the eastern coast of Hainan Island. *Cont. Shelf Res.* **2020**, *207*, 104209. [CrossRef]
4. Chen, C.; Lao, Q.; Chen, F.; Jin, G.; Li, J.; Zhu, Q. Isotope constraints on seasonal dynamics of nitrogen in Zhanjiang Bay, a typical mariculture bay in South China. *Acta Oceanol. Sin.* **2024**, *43*, 60–70. [CrossRef]

5. Zhou, F.; Wang, S.; Fang, H.; He, J.; Ye, L.; Ding, Z.; Li, C.; Chen, F.; Lu, X.; Chen, C.; et al. Distribution and sources of sedimentary organic matter in different aquaculture areas of northeastern Zhanjiang Bay using stable carbon and nitrogen isotopes. *Acta Oceanol. Sin.* **2024**, *43*, 38–48. [CrossRef]
6. Gu, B.; Ju, X.; Chang, J.; Ge, Y.; Vitousek, P.M. Integrated reactive nitrogen budgets and future trends in China. *Proc. Natl. Acad. Sci. USA* **2015**, *112*, 8792–8797. [CrossRef]
7. Xu, H.; Paerl, H.W.; Qin, B.; Zhu, G.; Gaoa, G. Nitrogen and phosphorus inputs control phytoplankton growth in eutrophic Lake Taihu, China. *Limnol. Oceanogr.* **2010**, *55*, 420–432. [CrossRef]
8. Dai, M.; Zhao, Y.; Chai, F.; Chen, M.; Chen, N.; Chen, Y.; Cheng, D.; Gan, J.; Guan, D.; Hong, Y.; et al. Persistent eutrophication and hypoxia in the coastal ocean. *Camb. Prism. Coast. Futures* **2023**, *1*, e19. [CrossRef]
9. Glibert, P.M.; Allen, J.I.; Artioli, Y.; Beusen, A.; Bouwman, L.; Harle, J.; Holmes, R.; Holt, J. Vulnerability of coastal ecosystems to changes in harmful algal blooms distribution in response e to climate change: Projections based on model analysis. *Glob. Change Biol.* **2014**, *20*, 3845–3858. [CrossRef] [PubMed]
10. Khangaonkar, T.; Nugraha, A.; Xu, W.; Long, W.; Bianucci, L.; Ahmed, A.; Mohamedali, T.; Pelletier, G. Analysis of hypoxia and sensitivity to nutrient pollution in Salish Sea. *J. Geophys. Res. Ocean.* **2018**, *123*, 4735–4761. [CrossRef]
11. Lao, Q.; Liu, S.; Ling, Z.; Jin, G.; Chen, F.; Chen, C.; Zhu, Q. External dynamic mechanisms controlling the periodic offshore blooms in Beibu Gulf. *J. Geophys. Res. Ocean.* **2023**, *128*, e2023JC019689. [CrossRef]
12. Verdegem, M.; Buschmann, A.H.; Latt, U.W.; Dalsgaard, A.J.; Lovatelli, A. The contribution of aquaculture systems to global aquaculture production. *J. World Aquac. Soc.* **2023**, *54*, 206–250. [CrossRef]
13. Williams, J.; Crutzen, P.J. Nitrous oxide from aquaculture. *Nat. Geosci.* **2010**, *3*, 143. [CrossRef]
14. Isada, T.; Abe, H.; Kasai, H.; Nakaoka, M. Dynamics of nutrients and colored dissolved organic matter absorption in a wetland-influenced subarctic coastal region of Northeastern Japan: Contributions from mariculture and eelgrass meadows. *Front. Mar. Sci.* **2021**, *8*, 711832. [CrossRef]
15. Bouwman, L.; Beusen, A.; Glibert, P.M.; Overbeek, C.; Pawlowski, M.; Herrera, J.; Mulsow, S.; Yu, R.; Zhou, M. Mariculture: Significant and expanding cause of coastal nutrient enrichment. *Environ. Res. Lett.* **2013**, *8*, 044026. [CrossRef]
16. Zhang, J.; Wu, W.; Li, Y.; Liu, Y.; Wang, X. Environmental effects of mariculture in China: An overall study of nitrogen and phosphorus loads. *Acta Oceanol. Sin.* **2022**, *41*, 4–11. [CrossRef]
17. Xiong, Y.; Gao, L.; Qu, L.; Xu, J.; Ma, Z.; Gao, G. The contribution of fish and seaweed mariculture to the coastal fluxes of biogenic elements in two important aquaculture areas, China. *Sci. Total Environ.* **2023**, *856*, 159056. [CrossRef]
18. Hu, Z.; Lee, J.W.; Chandran, K.; Kim, S.; Khanal, S.K. Nitrous oxide (N_2O) emission from aquaculture: A review. *Environ. Sci. Technol.* **2012**, *46*, 6470–6480. [CrossRef]
19. Liu, G.F.; Xu, P.; Wu, T.; Xu, Z.H.; Xu, G.C. Present condition of aquaculture nitrogen and phosphorus environmental pollution and future development strategy. *Jiangsu J. Agric. Sci.* **2018**, *34*, 225–233.
20. Go, Y.S.; Kim, C.S.; Lee, W.C.; Lee, D.H. A stable isotopic approach for quantifying aquaculture-derived organic matter deposition dynamics in the sediment of a coastal fish farm. *Mar. Pollut. Bull.* **2023**, *192*, 115132. [CrossRef]
21. Drizo, A.; Shaikh, M.O. An assessment of approaches and techniques for estimating water pollution releases from aquaculture production facilities. *Mar. Pollut. Bull.* **2023**, *196*, 115661. [CrossRef]
22. Zhuang, Y.; Li, Y.; Chen, L.; Jin, H.; Qi, D.; Chen, J. Biogeochemical and physical controls on ammonium accumulation on the Chukchi shelf, western Arctic Ocean. *Mar. Environ. Res.* **2023**, *190*, 106084. [CrossRef]
23. Troell, M.; Halling, C.; Neori, A.; Chopin, T.; Buschmann, A.H.; Kautsky, N.; Yarish, C. Integrated mariculture: Asking the right questions. *Aquaculture* **2003**, *226*, 69–90. [CrossRef]
24. Neori, A.; Chopin, T.; Troell, M.; Buschmann, A.H.; Kraemer, G.P.; Halling, C.; Shpigel, M.; Yarish, C. Integrated aquaculture: Rationale, evolution and state of the art emphasizing seaweed biofiltration in modern mariculture. *Aquaculture* **2004**, *231*, 361–391. [CrossRef]
25. Jiang, Z.; Liu, J.; Li, S.; Chen, Y.; Du, P.; Zhu, Y.; Liao, Y.; Chen, Q.; Shou, L.; Yan, X.; et al. Kelp cultivation effectively improves water quality and regulates phytoplankton community in a turbid, highly eutrophic bay. *Sci. Total Environ.* **2020**, *707*, 135561. [CrossRef] [PubMed]
26. Xu, S.; Yu, Z.; Zhou, Y.; Yue, S.; Liang, J.; Zhang, X. The potential for large-scale kelp aquaculture to counteract marine eutrophication by nutrient removal. *Mar. Pollut. Bull.* **2023**, *187*, 114513. [CrossRef]
27. Wankel, S.D.; Kendall, C.; Paytan, A. Using nitrate dual isotopic composition ($\delta^{15}N$ and $\delta^{18}O$) as a tool for exploring sources and cycling of nitrate in an estuarine system: Elkhorn Slough, California. *J. Geophys. Res. Biogeosci.* **2009**, *114*. [CrossRef]
28. Wankel, S.D.; Kendall, C.; Francis, C.A.; Paytan, A. Nitrogen sources and cycling in the San Francisco Bay Estuary: A nitrate dual isotopic composition approach. *Limnol. Oceanogr.* **2006**, *51*, 1654–1664. [CrossRef]
29. Kang, X.; Niu, Y.; Yu, H.; Gou, P.; Hou, Q.; Lu, X.; Wu, Y. Effect of rainfall-runoff process on sources and transformations of nitrate using a combined approach of dual isotopes, hydrochemical and Bayesian model in the Dagang River basin. *Sci. Total Environ.* **2022**, *837*, 155674. [CrossRef]

30. Zhong, X.; Yan, M.; Ning, X.; Yan, Z.; Xin, Y. Nitrate processing traced by nitrate dual isotopic composition in the early spring in the Changjiang (Yangtze River) Estuary and adjacent shelf areas. *Mar. Pollut. Bull.* **2020**, *161*, 111699. [CrossRef]
31. Tian, S.; Gaye, B.; Tang, J.; Luo, Y.; Li, W.; Lahajnar, N.; Dähnke, K.; Sanders, T.; Xiong, T.; Zhai, W.; et al. A nitrate budget of the Bohai Sea based on an isotope mass balance model. *Biogeosciences* **2022**, *19*, 2397–2415. [CrossRef]
32. Casciotti, K.L. Nitrogen and oxygen isotopic studies of the marine nitrogen cycle. *Annu. Rev. Mar. Sci.* **2016**, *8*, 379–407. [CrossRef] [PubMed]
33. Archana, A.; Thibodeau, B.; Geeraert, N.; Xu, M.N.; Kao, S.J.; Baker, D.M. Nitrogen sources and cycling revealed by dual isotopes of nitrate in a complex urbanized environment. *Water Res.* **2018**, *142*, 459–470. [CrossRef] [PubMed]
34. Divers, M.T.; Elliott, E.M.; Bain, D.J. Quantification of nitrate sources to an urban stream using dual nitrate isotopes. *Environ. Sci. Technol.* **2014**, *48*, 10580–10587. [CrossRef] [PubMed]
35. Guo, Z.; Yan, C.; Wang, Z.; Xu, F.; Yang, F. Quantitative identification of nitrate sources in a coastal peri-urban watershed using hydrogeochemical indicators and dual isotopes together with the statistical approaches. *Chemosphere* **2020**, *243*, 125364. [CrossRef]
36. Wang, X.; Zhang, Y.; Luo, M.; Xiao, K.; Wang, Q.; Tian, Y.; Qiu, W.; Xiong, Y.; Zheng, C.; Li, H. Radium and nitrogen isotopes tracing fluxes and sources of submarine groundwater discharge driven nitrate in an urbanized coastal area. *Sci. Total Environ.* **2021**, *763*, 144616. [CrossRef] [PubMed]
37. Chen, Y.; Chen, J.; Wang, Y.; Jiang, Y.; Zheng, M.; Qiu, Y.; Chen, M. Sources and transformations of nitrite in the Amundsen Sea in summer 2019 and 2020 as revealed by nitrogen and oxygen isotopes. *Acta Oceanol. Sin.* **2023**, *42*, 16–24. [CrossRef]
38. Yang, Z.; Chen, J.; Li, H.; Jin, H.; Gao, S.; Ji, Z.; Zhu, Y.; Ran, L.; Zhang, J.; Liao, Y.; et al. Sources of nitrate in Xiangshan Bay (China), as identified using nitrogen and oxygen isotopes. *Estuarine. Coast. Shelf Sci.* **2018**, *207*, 109–118. [CrossRef]
39. Yang, Z.; Chen, J.; Jin, H.; Li, H.; Ji, Z.; Li, Y.; Wang, B.; Cao, Z.; Chen, Q. Tracing nitrate sources in one of the world's largest eutrophicated bays (Hangzhou Bay): Insights from nitrogen and oxygen isotopes. *Acta Oceanol. Sin.* **2024**, *43*, 86–95. [CrossRef]
40. Pingping, K.; Peng, L.; Fuqiang, W. Use of multiple isotopes to evaluate the impact of mariculture on nutrient dynamics in coastal groundwater. *Environ. Sci. Pollut. Res.* **2019**, *26*, 12399–12411. [CrossRef]
41. Kendall, C. Tracing nitrogen sources and cycling in catchments. In *Isotope Tracers in Catchment Hydrology*; Elsevier: Amsterdam, The Netherlands, 1998; pp. 519–576.
42. Xue, D.; Botte, J.; De Baets, B.; Accoe, F.; Nestler, A.; Taylor, P.; Van Cleemput, O.; Berglund, M.; Boeckx, P. Present limitations and future prospects of stable isotope methods for nitrate source identification in surface-and groundwater. *Water Res.* **2009**, *43*, 1159–1170. [CrossRef] [PubMed]
43. Chen, F.; Lao, Q.; Jia, G.; Chen, C.; Zhu, Q.; Zhou, X. Seasonal variations of nitrate dual isotopes in wet deposition in a tropical city in China. *Atmos. Environ.* **2019**, *196*, 1–9. [CrossRef]
44. Granger, J.; Sigman, D.M.; Lehmann, M.F.; Tortell, P.D. Nitrogen and oxygen isotope fractionation during dissimilatory nitrate reduction by denitrifying bacteria. *Limnol. Oceanogr.* **2008**, *53*, 2533–2545. [CrossRef]
45. Granger, J.; Sigman, D.M.; Needoba, J.A.; Harrison, P.J. Coupled nitrogen and oxygen isotope fractionation of nitrate during assimilation by cultures of marine phytoplankton. *Limnol. Oceanogr.* **2004**, *49*, 1763–1773. [CrossRef]
46. Sigman, D.M.; Granger, J.; DiFiore, P.J.; Lehmann, M.M.; Ho, R.; Cane, G.; Van Geen, A. Coupled nitrogen and oxygen isotope measurements of nitrate along the eastern North Pacific margin. *Glob. Biogeochem. Cycles* **2005**, *19*. [CrossRef]
47. Sigman, D.M.; DiFiore, P.J.; Hain, M.P.; Deutsch, C.; Wang, Y.; Karl, D.M.; Knapp, A.N.; Lehmann, M.F.; Pantoja, S. The dual isotopes of deep nitrate as a constraint on the cycle and budget of oceanic fixed nitrogen. *Deep Sea Res. Part I Oceanogr. Res. Pap.* **2009**, *56*, 1419–1439. [CrossRef]
48. Chen, C.; Lao, Q.; Shen, Y.; Jin, G.; Chen, F.; Su, Q.; Lei, X.; Zhou, X.; Lu, X.; Zhu, Q.; et al. Comparative study of nitrogen cycling between a bay with riverine input and a bay without riverine input, inferred from stable isotopes. *Front. Mar. Sci.* **2022**, *9*, 885037. [CrossRef]
49. Bu, D.; Zhu, Q.; Li, J.; Huang, J.; Zhuang, Y.; Yang, W.; Qi, D. Mariculture may intensify eutrophication but lower N/P ratios: A case study based on nutrients and dual nitrate isotope measurements in Sansha Bay, southeastern China. *Front. Mar. Sci.* **2024**, *11*, 1351657. [CrossRef]
50. Li, Y.; Jin, H.; Chen, J.; Wang, D.; Yang, Z.; Wang, B.; Zhuang, Y.; Wang, R. Nitrogen removal through sediment denitrification in the Yangtze Estuary and its adjacent East China Sea: A nitrate limited process during summertime. *Sci. Total Environ.* **2021**, *795*, 148616. [CrossRef]
51. Wang, G.; Han, A.; Chen, L.; Tan, E.; Lin, H. Fluxes of dissolved organic carbon and nutrients via submarine groundwater discharge into subtropical Sansha Bay, China. *Estuar. Coast. Shelf Sci.* **2018**, *207*, 269–282. [CrossRef]
52. Zhu, F.; Shi, Z.Z.; Ling, X.W.; Xia, Y.J.; Li, Y.; Weng, Y.C.; Liu, Y.X. Relationship between cage aquaculture and environmental quality in Sansha Bay of Ningde. *Mar. Sci. Bull.* **2013**, *32*, 171–177.
53. Lin, H.; Chen, Z.; Hu, J.; Cucco, A.; Zhu, J.; Sun, Z.; Huang, L. Numerical simulation of the hydrodynamics and water exchange in Sansha Bay. *Ocean Eng.* **2017**, *139*, 85–94. [CrossRef]

54. Lao, Q.; Zhang, S.; Li, Z.; Chen, F.; Zhou, X.; Jin, G.; Huang, P.; Deng, Z.; Chen, C.; Zhu, Q.; et al. Quantification of the seasonal intrusion of water masses and their impact on nutrients in the Beibu Gulf using dual water isotopes. *J. Geophys. Res. Ocean.* **2022**, *127*, e2021JC018065. [CrossRef]
55. Zhang, Z.; Lei, L.; Wang, F.; Li, R.; Li, C.; Huang, Y.; Mu, J. Assessment of Carbon Sequestration Potential of Mariculture in Sansha Bay and Spatial Pattern Analysis. *Ocean Dev. Manag.* **2024**, *41*, 28–37.
56. Han, A.; Kao, S.J.; Lin, W.; Lin, Q.; Han, L.; Zou, W.; Tan, E.; Lai, Y.; Ding, G.; Lin, H. Nutrient budget and biogeochemical dynamics in Sansha Bay, China: A coastal bay affected by intensive mariculture. *J. Geophys. Res. Biogeosci.* **2021**, *126*, e2020JG006220. [CrossRef]
57. McIlvin, M.R.; Altabet, M.A. Chemical conversion of nitrate and nitrite to nitrous oxide for nitrogen and oxygen isotopic analysis in freshwater and seawater. *Anal. Chem.* **2005**, *77*, 5589–5595. [CrossRef] [PubMed]
58. Granger, J.; Sigman, D.M. Removal of nitrite with sulfamic acid for nitrate N and O isotope analysis with the denitrifier method. *Rapid Commun. Mass Spectrom.* **2009**, *23*, 3753–3762. [CrossRef]
59. Davis, P.; Syme, J.; Heikoop, J.; Fessenden-Rahn, J.; Perkins, G.; Newman, B.; Chrystal, A.E.; Hagerty, S.B. Quantifying uncertainty in stable isotope mixing models. *J. Geophys. Res. Biogeosci.* **2015**, *120*, 903–923. [CrossRef]
60. Zhang, M.; Zhi, Y.; Shi, J.; Wu, L. Apportionment and uncertainty analysis of nitrate sources based on the dual isotope approach and a Bayesian isotope mixing model at the watershed scale. *Sci. Total Environ.* **2018**, *639*, 1175–1187. [CrossRef]
61. Lao, Q.; Liu, G.; Gao, J.; Shen, Y.; Su, Q.; Chen, C.; Chen, F. Seasonal Sources and Cycling of Nitrogen Revealed by Stable Isotopes in the Northeastern Beibu Gulf, China. *J. Mar. Sci. Eng.* **2021**, *9*, 1123. [CrossRef]
62. Torres−Martínez, J.A.; Mora, A.; Knappett, P.S.; Ornelas−Soto, N.; Mahlknecht, J. Tracking nitrate and sulfate sources in groundwater of an urbanized valley using a multi-tracer approach combined with a Bayesian isotope mixing model. *Water Res.* **2020**, *182*, 115962. [CrossRef]
63. Moore, J.W.; Semmens, B.X. Incorporating uncertainty and prior information into stable isotope mixing models. *Ecol. Lett.* **2008**, *11*, 470–480. [CrossRef] [PubMed]
64. Wang, B.; Sun, X.; Wei, Q.; Xie, L. A new method and application for the evaluation of eutrophication in China's near-shore sea area. *Haiyang Xuebao* **2012**, *34*, 61–66. (In Chinese)
65. Feng, Y.Y.; Hou, L.C.; Ping, N.X.; Ling, T.D.; Kyo, C.I. Development of mariculture and its impacts in Chinese coastal waters. *Rev. Fish Biol. Fish.* **2004**, *14*, 1–10. [CrossRef]
66. Morris, K.A.; Saetre, P.; Norton, U.; Stark, J.M. Plant community effects on soil moisture and nitrogen cycling in a semi-arid ecosystem. *Biogeochemistry* **2022**, *159*, 215–232. [CrossRef]
67. Xie, B.; Huang, J.; Huang, C.; Wang, Y.; Shi, S.; Huang, L. Stable isotopic signatures ($\delta^{13}C$ and $\delta^{15}N$) of suspended particulate organic matter as indicators for fish cage culture pollution in Sansha Bay, China. *Aquaculture* **2020**, *522*, 735081. [CrossRef]
68. Duan, Q.; Mai, K.; Zhong, H.; Si, L.; Wang, X. Studies on the nutrition of the large yellow croaker, Pseudosciaena crocea R. I: Growth response to graded levels of dietary protein and lipid. *Aquac. Res.* **2001**, *32*, 46–52. [CrossRef]
69. Wang, Y.; Guo, X.; Wang, G.; Wang, L.; Huang, T.; Li, Y.; Wang, Z.; Dai, M. Assessment of nutrient cycling in an intensive mariculture system. *Mar. Pollut. Bull.* **2024**, *209*, 117085. [CrossRef] [PubMed]
70. Roleda, M.Y.; Hurd, C.L. Seaweed nutrient physiology: Application of concepts to aquaculture and bioremediation. *Phycologia* **2019**, *58*, 552–562. [CrossRef]
71. Yu, X.; Liu, J.; Chen, X.; Huang, D.; Yu, T.; Peng, T.; Du, J. Submarine groundwater-derived inorganic and organic nutrients vs. mariculture discharge and river contributions in a typical mariculture bay. *J. Hydrol.* **2022**, *613*, 128342. [CrossRef]
72. van der Schatte Olivier, A.; Jones, L.; Vay, L.L.; Christie, M.; Wilson, J.; Malham, S.K. A global review of the ecosystem services provided by bivalve aquaculture. *Rev. Aquac.* **2020**, *12*, 3–25. [CrossRef]
73. Nederlof, M.A.; Verdegem, M.C.; Smaal, A.C.; Jansen, H.M. Nutrient retention efficiencies in integrated multi-trophic aquaculture. *Rev. Aquac.* **2022**, *14*, 1194–1212. [CrossRef]
74. Ji, W.; Yokoyama, H.; Fu, J.; Zhou, J. Effects of intensive fish farming on sediments of a temperate bay characterised by polyculture and strong currents. *Aquac. Rep.* **2021**, *19*, 100579. [CrossRef]
75. Mengis, M.; Schif, S.L.; Harris, M.; English, M.C.; Aravena, R.; Elgood, R.J.; MacLean, A. Multiple geochemical and isotopic approaches for assessing ground water NO3− elimination in a riparian zone. *Groundwater* **1999**, *37*, 448–457. [CrossRef]
76. Tian, S.; Gaye, B.; Tang, J.; Luo, Y.; Lahajnar, N.; Daehnke, K.; Sanders, T.; Xiong, T.; Zhai, W.; Emeis, K.C. Nitrate regeneration and loss in the Central Yellow Sea bottom water revealed by nitrogen isotopes. *Front. Mar. Sci.* **2022**, *9*, 834953. [CrossRef]
77. Wu, J.; Hong, Y.; Liu, X.; Hu, Y. Variations in nitrogen removal rates and microbial communities over sediment depth in Daya Bay, China. *Environ. Pollut.* **2021**, *286*, 117267. [CrossRef]
78. Zhuang, Y.; Jin, H.; Cai, W.J.; Li, H.; Qi, D.; Chen, J. Extreme nitrate deficits in the western Arctic Ocean: Origin, decadal changes, and implications for denitrification on a polar marginal shelf. *Glob. Biogeochem. Cycles* **2022**, *36*, e2022GB007304. [CrossRef]

79. Ahad, J.M.; Ganeshram, R.S.; Spencer, R.G.; Uher, G.; Upstill−Goddard, R.C.; Cowie, G.L. Evaluating the sources and fate of anthropogenic dissolved inorganic nitrogen (DIN) in two contrasting North Sea estuaries. *Sci. Total Environ.* **2006**, *372*, 317–333. [CrossRef]
80. Chen, F.; Chen, J.; Jia, G.; Jin, H.; Xu, J.; Yang, Z.; Zhuang, Y.; Liu, X.; Zhang, H. Nitrate $\delta^{15}N$ and $\delta^{18}O$ evidence for active biological transformation in the Changjiang Estuary and the adjacent East China Sea. *Acta Oceanol. Sin.* **2013**, *32*, 11–17.
81. Glibert, P.M.; Wilkerson, F.P.; Dugdale, R.C.; Raven, J.A.; Dupont, C.L.; Leavitt, P.R.; Parker, A.E.; Burkholder, J.M.; Kana, T.M. Pluses and minuses of ammonium and nitrate uptake and assimilation by phytoplankton and implications for productivity and community composition, with emphasis on nitrogen-enriched conditions. *Limnol. Oceanogr.* **2016**, *61*, 165–197. [CrossRef]
82. Ye, F.; Jia, G.; Xie, L.; Wei, G.; Xu, J. Isotope constraints on seasonal dynamics of dissolved and particulate N in the Pearl River Estuary, south China. *J. Geophys. Res. Ocean.* **2016**, *121*, 8689–8705.
83. Xue, D.; De Baets, B.; Van Cleemput, O.; Hennessy, C.; Berglund, M.; Boeckx, P. Use of a Bayesian isotope mixing model to estimate proportional contributions of multiple nitrate sources in surface water. *Environ. Pollut.* **2012**, *161*, 43–49. [CrossRef] [PubMed]
84. Chen, F.; Deng, Z.; Lao, Q.; Bian, P.; Jin, G.; Zhu, Q.; Zhou, X.; Chen, C. Nitrogen cycling across a salinity gradient from the pearl river estuary to offshore: Insight from nitrate dual isotopes. *J. Geophys. Res. Biogeosci.* **2022**, *127*, e2022JG006862. [CrossRef]
85. Kendall, C.; Elliott, E.M.; Wankel, S.D. Tracing anthropogenic inputs of nitrogen to ecosystems. In *Stable Isotopes in Ecology and Environmental Science*; Blackwell Publishing Ltd.: Oxford, UK, 2007; pp. 375–449.

Disclaimer/Publisher's Note: The statements, opinions and data contained in all publications are solely those of the individual author(s) and contributor(s) and not of MDPI and/or the editor(s). MDPI and/or the editor(s) disclaim responsibility for any injury to people or property resulting from any ideas, methods, instructions or products referred to in the content.